

## ON THE DEVELOPMENT OF TRANSVERSE RIDGES ON ROCK GLACIERS

By DEBORAH S. LOEWENHERZ,\* CHRISTOPHER J. LAWRENCE, and RICHARD L. WEAVER

(Department of Theoretical and Applied Mechanics, University of Illinois at Urbana-Champaign,  
Urbana, Illinois 61801, U.S.A.)

**ABSTRACT.** The stability of a low Reynolds number flow on an inclined plane is investigated with respect to modelling the initiation of transverse wave-like ridges which commonly occur on the surfaces of rock-glacier forms. In accordance with field observations indicating the presence of stratification in rock glaciers, two models of rock-glacier structure are considered, each stratified and possessing a lower layer which is treated as a Newtonian fluid. An upper, less compliant layer is treated, alternatively, as a Newtonian fluid of viscosity greater than that of the lower layer, or as an elastic solid under longitudinal compression induced by a decrease in the slope of the underlying incline. A linear stability analysis is used to examine the behaviour of each of the proposed models, and both are found to generate instabilities at wavelengths comparable to those associated with transverse surficial ridges on rock glaciers. The growth rates of a flow disturbance predicted by the viscous-stratified model appear to be too slow to account fully for the development of wave forms of finite amplitude, suggesting that other mechanisms are involved in the amplification of an initial disturbance. The results of the stability analysis of the elastic lamina model indicate that finite surficial ridges may develop on rock glaciers as a product of a buckling instability in the surface region if there is a decrease in the slope of the underlying incline. Both of the analyses illustrate that transverse ridges can occur on the surface of a rock glacier in the absence of any variations in debris supply to the system. The results further imply that the use of these features in the paleoreconstruction of Holocene climatic conditions must entail an assessment of the relative roles of external climatically driven forcing *versus* internal rheologically derived instability.

### 1. INTRODUCTION

Rock glaciers are depositional forms composed primarily of debris with some interstitial ice, which are found in periglacial environments, and which, while active, exhibit down-slope movement. They are generally either lobate or tongue-shaped in planform, and often possess a quite characteristic micro-relief consisting of transverse ridges and furrows on their upper surfaces. A number of excellent photographic illustrations of these features are available in the literature, and the reader is referred particularly to the classic study of rock glaciers in Alaska by Wahrhaftig and Cox (1959), the photo-interpretive analysis of rock glaciers published by Outcalt and Benedict (1965), or the recent review of rock-glacier research by Barsch (1988) for pictorial examples of these forms.

Active rock glaciers have been identified in a variety of alpine environments, including the Sierra Nevada (Kesseli, 1941), the Andes (Lliboutry, 1953; Corte, 1976), the Himalaya (Mayewski and others, 1981), the Swiss Alps

(Chaix, 1923), the Alaska Range (Wahrhaftig and Cox, 1959), the Brooks Range, Alaska (Calkin and others, 1987), and throughout the American and Canadian Rockies (e.g. Brown, 1925; Richmond, 1952; Potter, 1972; Luckman and Crockett, 1978; Harris, 1981). Active forms are also found in certain polar environments such as Svalbard in Arctic Norway (Swett and others, 1980) and Victoria Land, Antarctica (Mayewski and Hassinger, 1981). The observed distribution of active rock glaciers indicates that their development is favored in mountainous areas characterized by temperature and moisture conditions which are sufficient for the production of an abundant supply of rock debris and the accumulation of interstitial ice, but which cannot support the formation of an ice glacier (Madole, 1972; Benedict, 1973; Morris, 1981; Olyphant, 1985). This is further corroborated by the presence of relict (fossil) rock glaciers in areas contiguous with the limits of late Pleistocene glaciation (e.g. Blagbrough and Farkas, 1968; Birkeland, 1973; Mahaney, 1980).

The rock glaciers observed via both field and photogrammetric studies are generally grouped into two classes. The first class includes the "lobate" or "valley-wall" forms which extend as single or multiple lobes from the bases of talus deposits along the sides of presently or previously glaciated valleys. They are commonly much wider than they are long and widths of up to 3000 m, with an associated length of 500 m, have been reported (Wahrhaftig and Cox, 1959). Average widths, however, are more apt to be between 100 and 500 m (Madole, 1972; Barsch, 1977). The "tongue-shaped" or "valley-floor" forms which are generally found in cirques below end moraines or below existing glaciers constitute the second class of rock glacier. They exhibit average lengths of 350–1000 m and widths of 40–150 m (Madole, 1972; Barsch, 1977), although forms having lengths of the order of 1600 m (e.g. Potter, 1972) are frequently observed. The distinction between the two classes of features is not necessarily entirely morphological, and numerous speculations regarding differences in the origin of each type have been presented.

Field observations of the internal structure of both classes of rock glacier indicate that they usually consist of an upper layer of coarse, blocky or angular debris, and a lower layer composed primarily of silt- and clay-sized particles (Wahrhaftig and Cox, 1959; White, 1971; Barsch and others, 1979). The coarse upper layer tends to be quite thin (sometimes no more than 2–3 m) compared to the total thickness of the rock glacier, which is often 35–50 m (Wahrhaftig and Cox, 1959). Interstitial ice appears to be present in both the upper and lower layers (White, 1971; Barsch, 1977; Barsch and others, 1979), and larger bodies of ice in the form of lenses or even possible ice cores have been observed in the lower layers of some features (e.g. Brown, 1925; Kesseli, 1941; Potter, 1972; Benedict, 1973; White, 1975). This latter characteristic has led many researchers to speculate that all rock glaciers are merely debris-covered ice glaciers and that their movement is derived solely from the creep of the ice core (e.g. Brown, 1925; Kesseli, 1941; Whalley, 1974; Corte, 1976). Other researchers have suggested that "tongue-shaped" rock glaciers

\* Present address: Department of Geology and Geophysics, University of California at Berkeley, Berkeley, California 94720, U.S.A.

represent debris-covered relict ice glaciers and/or ice-cored moraines, while the lobate forms are constructed entirely of rock debris cemented with interstitial ice (Outcalt and Benedict, 1965; Madole, 1972). Recent field evidence, however, fails to support fully either of these conjectures (e.g. Barsch and others, 1979; Johnson, 1981; Barsch, 1987; King and others, 1987) and suggests that, although ice cores may be present in some rock glacier-type features, they represent the exception rather than the norm. Additionally, many of the rock glaciers which were originally characterized as having massive ice cores, such as the Hurricane Basin rock glacier in the San Juan Mountains, Colorado (Brown, 1925), the Galena Creek rock glacier in the Absaroka Mountains, Wyoming (Potter, 1972), and the Grubengletscher rock glacier in the Swiss Alps (Whalley, 1974), have subsequently been found to be composed primarily of rock debris and interstitial ice (Barsch and others, 1979; Haerberli and others, 1979; Barsch, 1987; King and others, 1987).

Field and photogrammetric measurements indicate that active rock glaciers are currently moving down-slope at average speeds of 1–160 cm/year ( $0.3 \times 10^{-9} - 5 \times 10^{-8}$  m/s) (White, 1971; Barsch, 1977; Hassinger and Mayewski, 1983; Benedict and others, 1986). Various flow mechanisms have been suggested over the years and the reader is referred to discussion in the papers by Wahrhaftig and Cox (1959), Potter (1972), and Whalley (1974) for overviews of the early theories. In recent years, it has generally been the consensus that rock glaciers creep down-slope as a result of the deformation of the interstitial ice matrix driven by the weight of the rock debris. This hypothesis was seriously questioned by Whalley (1974), who proposed that the shear strength of a rock/ice composite would far exceed the maximum shear stress associated with observed rock glaciers based on their thickness and the slope of their surface, thus indicating that substantial ice cores were necessary for rock-glacier movement. The results of Whalley's analysis appeared to provide some support for his proposition; however, they were based on rather inadequate data regarding the mechanical properties of rock debris/ice mixtures and so he considered the analysis to be inconclusive. Furthermore, as mentioned above, recent investigations have shown that some of the field examples of active rock glaciers which Whalley used to support his theory actually represent ice-cemented rather than ice-cored forms. Thus, current evidence continues to favor the hypothesis that many rock glaciers do move down-slope solely as a result of the continuous deformation of the rock/ice composite material, although it is recognized that in some cases other mechanisms such as basal sliding (Fisch and others, 1978) or the creep of a remnant ice core (White, 1981) may also contribute to the movement.

Perhaps the most distinctive characteristic of rock-glacier forms is the quite striking pattern of micro-relief which occurs on the upper surface. This micro-relief usually consists of a series of transverse ridges and furrows which occur parallel to the front of the rock glacier. These features often have heights of 1–6 m (Wahrhaftig and Cox, 1959; White, 1976), and the ridge crests are spaced from 2 to 50 m apart (Wahrhaftig and Cox, 1959; Potter, 1972). A variety of mechanisms for the development of ridges has been proposed, including: (1) the differential movement of discrete layers of debris (Ives, 1940); (2) "shearing" or "compression" within the rock glacier which results from a decrease in basal slope and an associated increase in the thickness of the feature (Wahrhaftig and Cox, 1959; Potter, 1972); and (3) debris-input variations resulting from changes in talus production (Barsch, 1977). It seems to be generally accepted that the ridges and furrows are to some extent an expression of the down-slope movement of a rock glacier due to the similarity of their appearance to surficial features observed on other very viscous flows such as lava flows and mud flows; however, their rheological significance is still an unresolved issue. Although it is possible that external factors such as variations in debris input may contribute to the formation of surficial ridges, their ubiquitous presence demands that internal mechanisms for their development be considered. In the analysis that follows, we propose two rheological models for describing the structure of a rock glacier and evaluate the stability of parallel flow with respect to small-amplitude disturbances.

We will thereby assess the conditions under which an unstable flow configuration which is capable of generating wave forms of finite amplitude can exist in the absence of variations in debris supply.

The simplest model of rock-glacier deformation is that of a single layer of fluid flowing down an inclined plane of infinite extent. This model was used by Wahrhaftig and Cox (1959) to assess the Newtonian viscosity of observed rock glaciers, and also by Olyphant (1983) to compare steady-state configurations obtained using Newtonian and non-Newtonian flow laws. However, the results of stability analyses of single-fluid layers using both Newtonian (e.g. Benjamin, 1957; Yih, 1963) and non-Newtonian (e.g. Thompson, 1979) constitutive assumptions indicate that such flows are stable to infinitesimal disturbances at the low Reynolds numbers associated with rock glaciers, implying that wave-like ridges could not be generated as an internal product of such flows. Furthermore, as mentioned previously, field investigations of the internal structure of rock glaciers indicate that they tend to be characterized by a stratified composition, which can most simply be resolved into two distinct layers of debris. In most cases, the upper layer is relatively thin and is composed of coarse material, while the lower layer represents the bulk of the mass of the rock glacier, and is made up of fine debris. These observations suggest the use of a flow model consisting of two discrete layers of material, each material having distinct physical properties. Therefore, in the succeeding analysis we will investigate the flow of a stratified system composed of two layers of fluid having similar densities but differing viscosities. We will also consider a flow configuration consisting of a single layer of fluid overlain by a thin elastic lamina. In both these models, the fluid will be specified as Newtonian in nature. An alternative approach would be the use of a power-law constitutive relationship such as the one employed by Olyphant (1983, 1987) in numerical simulations of rock-glacier behavior. However, there is no clear indication via laboratory or field evidence that a rock debris/ice composite material would behave as a non-Newtonian fluid at the extremely low shear rates found in rock glaciers. Therefore, we have chosen a Newtonian viscous model for describing the overall deformation of the features, as this represents the most simple and least arbitrary constitutive model of a continuously deforming medium.

## 2. TWO-FLUID LAYER MODEL

We will first consider the flow of a system consisting of two layers of fluid on an incline of constant declivity. In accordance with the observed internal structure of rock glaciers, the mass densities of the layers will be taken as equal, but their viscosities will be allowed to differ. As discussed in the preceding section, a linear viscous constitutive model is chosen to characterize the creep of the ice/debris composite material. The stability of this flow configuration has been examined in detail by Loewenherz and Lawrence (1988, in press), so we will refrain from repeating that analysis in full. Only a general formulation of the stability problem and those conclusions of relevance for the modelling of rock glaciers will be presented here.

The equations governing the flow of an incompressible Newtonian fluid are the Navier–Stokes equations. By specifying appropriate length, viscosity, velocity, body force per unit mass, time, and pressure scales ( $L, N, U, F, T, P$ , respectively) of the form

$$L = d_2; \quad N = \mu_2; \quad U = \frac{\rho g \sin \theta d_2^2}{\mu_2}; \quad F = g \sin \theta \tag{2.1}$$

$$T = \frac{L}{U} = \frac{\mu_2}{\rho g d_2 \sin \theta}; \quad P = \rho g d_2 \sin \theta$$

in which  $d_2$  is the thickness of the lower layer of the rock glacier (with reference to Figure 1),  $g$  is the acceleration due to gravity,  $\mu_2$  is the viscosity of the lower layer,  $\rho$  is the density of the fluid, and  $\theta$  is the characteristic angle of inclination of the underlying slope, the Navier–Stokes equations can be written in dimensionless form as

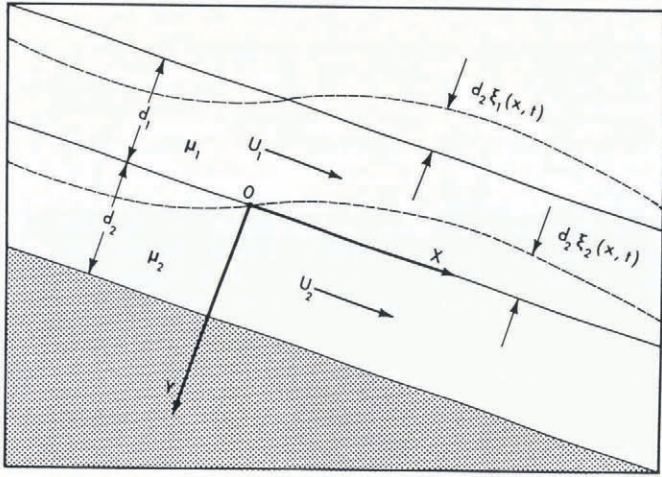


Fig. 1. Coordinate system for two-fluid layer model.

$$u_\alpha = U_\alpha + \epsilon u'_\alpha \tag{2.8}$$

$$v_\alpha = \epsilon v'_\alpha \tag{2.9}$$

$$p_\alpha = P + \epsilon p'_\alpha \tag{2.10}$$

where  $\epsilon \ll 1$  measures the small disturbance from the base flow, the primed quantities represent the perturbation, and  $\alpha$  takes on the values 1 and 2, thereby indicating the fluid layer under consideration. Substitution of Equations (2.8)–(2.10) into the momentum Equation (2.4) yields equations for the perturbation given by

$$\epsilon p'_{\alpha,x} = \mu_\alpha \nabla^2 (U_\alpha + \epsilon u'_\alpha) + 1 \tag{2.11}$$

$$(P + \epsilon p'_\alpha)_{,y} = \epsilon \mu_\alpha \nabla^2 v'_\alpha + \cot \theta. \tag{2.12}$$

The incompressibility condition suggests the use of a stream function  $\psi$  which is defined so that

$$\psi_{\alpha,y} = u'_\alpha; \quad \psi_{\alpha,x} = -v'_\alpha. \tag{2.13}$$

Using this representation for the components of the velocity perturbation, and recognizing that  $U_\alpha$  and  $P$  identically satisfy the equations governing the base flow, Equations (2.11)–(2.12) can be reduced to a pair of biharmonic equations

$$\nabla^4 \psi_\alpha = 0 \tag{2.14}$$

governing the stream function of the perturbation.

At the lower boundary, given by the dimensionless coordinate  $y = 1$ , a kinematic no-slip condition is applied, which in the terms of the stream functions is written as

$$(2i) \quad \psi_2 = 0 \quad \text{at } y = 1$$

$$(2ii) \quad \psi_{2,y} = 0 \quad \text{at } y = 1.$$

At the interface between the two fluid layers,  $y = \xi_2$ , the kinematic interface continuity condition is  $DF/Dt = 0$ , with  $F = y - \xi_2(x,t)$  defined so as to vanish on the interface. As indicated in Figure 1,  $\xi_2$  represents the dimensionless displacement of the interface from its unperturbed location at  $y = 0$ . The interface continuity condition may be expanded in Taylor series around  $y = 0$  and linearized to order  $\epsilon$  and yields

$$(2iii) \quad \xi_{2,t} + \xi_{2,x} U_2 = -\psi_{2,x} \quad \text{at } y = 0$$

$$(2iv) \quad \xi_{2,t} + \xi_{2,x} U_1 = -\psi_{1,x} \quad \text{at } y = 0.$$

Continuity of the  $x$ -component of material velocity across the interface becomes, upon a similar linearization,

$$(2v) \quad \xi_2 U_{1,y} + \psi_{1,y} = \xi_2 U_{2,y} + \psi_{2,y} \quad \text{at } y = 0.$$

The shear traction and normal traction continuity conditions are also linearized to give

$$(2vi) \quad \xi_2 U_{1,y,y} + \psi_{1,y,y} - \psi_{1,x,x} = M(\xi_2 U_{2,y,y} + \psi_{2,y,y} - \psi_{2,x,x}) \tag{2vi}$$

at  $y = 0$

$$(2vii) \quad p'_1 + 2\mu_1 \psi_{1,y,x} = p'_2 + 2\mu_2 \psi_{2,y,x} \quad \text{at } y = 0.$$

At the upper surface ( $y = -D + \xi_1$ ) the kinematic condition requiring continuity of the fluid/air interface is again applied. When linearized to order  $\epsilon$ , it yields

$$(2viii) \quad \xi_{1,t} + \xi_{1,x} U_1 = -\psi_{1,x} \quad \text{at } y = -D.$$

Finally, the linearized forms of the shear stress and normal stress boundary conditions at the free surface are

$$(2ix) \quad \xi_1 U_{1,y,y} + \psi_{1,y,y} - \psi_{1,x,x} = 0 \quad \text{at } y = -D$$

$$(2x) \quad \xi_1 P_{,y} + p'_1 + 2\mu_1 \psi_{1,x,y} = 0 \quad \text{at } y = -D.$$

A Fourier integral transform is now invoked to express the governing equations and boundary conditions in terms of a continuous superposition of Fourier modes. The

$$\text{Re} \sin \theta (u_l + u \cdot \nabla u) = -\nabla p + \mu \nabla^2 u + e_x + \cot \theta e_y \tag{2.2}$$

$$\nabla \cdot u = 0$$

where  $\text{Re}$  is the Reynolds number defined by

$$\text{Re} = \frac{\rho U L}{N} = \frac{\rho^2 g d_2^3 \sin \theta}{\mu_2^2} = \frac{U^2}{g d_2 \sin \theta}, \tag{2.3}$$

$u$  is the dimensionless material velocity of the fluid,  $p$  is the dimensionless pressure,  $\mu$  is the dimensionless viscosity, and  $e_x + e_y \cot \theta$  is the dimensionless body force due to gravity. Estimating the characteristic velocity of a rock glacier to be approximately 30 cm/year ( $10^{-8}$  m/s), its thickness to be about 40 m and its basal slope to be about 0.2 rad, a typical Reynolds number for a rock glacier is found to be of the order of  $10^{-18}$  (dimensionless). The flow of a rock glacier is therefore a low Reynolds number flow and the left-hand side of Equation (2.2) may be neglected. The equations governing the flow field can consequently be written in the simplified form

$$\nabla p = \mu \nabla^2 u + e_x + e_y \cot \theta \tag{2.4}$$

$$\nabla \cdot u = 0.$$

Upon imposition of boundary conditions requiring that the upper surface be stress-free, the lower surface has vanishing fluid velocity and the fluid–fluid interface has continuous velocity and traction, the parallel-flow solution (hereafter referred to as the base flow) can be established to be

$$u_\alpha = \frac{1}{2} + D - \frac{1}{\mu_\alpha} \left( \frac{1}{2} y^2 + D y \right) \equiv U_\alpha \tag{2.5}$$

$$v_\alpha = 0$$

where the subscript  $\alpha$  takes values 1 and 2, respectively, for the upper and lower layers in which the dimensionless viscosities are  $\mu_1 = M^{-1}$  and  $\mu_2 = 1$ ,  $u$  and  $v$  refer to the  $x$ - and  $y$ -components of fluid velocity, and  $M$  and  $D$  represent viscosity and thickness ratios defined as

$$D = \frac{d_1}{d_2} \quad M = \frac{\mu_2}{\mu_1}. \tag{2.6}$$

The expression for the base pressure is the same in each fluid, i.e.

$$p = \cot \theta (y + D) \equiv P \tag{2.7}$$

and is equivalent to a hydrostatic pressure distribution.

Perturbations of the base-flow solution can now be considered by representing the flow field in the form

transform is defined such that each mode is of the form

$$\begin{aligned} \psi_\alpha &= \phi_\alpha(y)\exp(ikx - i\omega t) \\ p'_\alpha &= q_\alpha(y)\exp(ikx - i\omega t) \\ \xi_\alpha &= \eta_\alpha\exp(ikx - i\omega t) \end{aligned} \tag{2.15}$$

where  $k$  is the dimensionless wave number and  $c$  is the dimensionless wave speed, with  $\omega = ck$ . The Fourier transforms of the governing Equations (2.14) are

$$k^4\phi_\alpha - 2k^2\phi''_\alpha + \phi'''_\alpha = 0 \tag{2.16}$$

where the primes now indicate derivatives with respect to  $y$ . The solutions of these governing equations are of the general form

$$\phi_\alpha(y) = A_\alpha \cosh ky + B_\alpha \sinh ky + C_\alpha k y \cosh ky + D_\alpha k y \sinh ky \tag{2.17}$$

in terms of the eight as yet unspecified constants  $A_\alpha$ ,  $B_\alpha$ ,  $C_\alpha$  and  $D_\alpha$ .

The pressure perturbation can be described in terms of the stream-function perturbation by taking a Fourier transform of Equation (2.11) to obtain

$$q_\alpha = \frac{\mu_\alpha}{ik}(\phi'''_\alpha - k^2\phi'_\alpha). \tag{2.18}$$

Upon substitution of Equations (2.17) and (2.18) into conditions (2i-2x), and evaluation of the base-flow velocities and pressures as given by Equations (2.5) and (2.7), a linear system of ten equations in ten unknowns (i.e. the eight coefficients and the two interface displacements  $\eta_\alpha$ ) is obtained:

$$(2ia) \quad A_2 \cosh k + B_2 \sinh k + C_2 k \cosh k + D_2 k \sinh k = 0$$

$$(2iia) \quad A_2 \sinh k + B_2 \cosh k + C_2 (\cosh k + k \sinh k) + D_2 (\sinh k + k \cosh k) = 0$$

$$(2iiaa) \quad \left(\frac{1}{2} + D - c\right)\eta_2 + A_2 = 0$$

$$(2iva) \quad \left(\frac{1}{2} + D - c\right)\eta_2 + A_1 = 0$$

$$(2va) \quad \frac{-D(M-1)}{k}\eta_2 + B_1 + C_1 - B_2 - C_2 = 0$$

$$(2via) \quad A_1 + D_1 = M(A_2 + D_2)$$

$$(2viiia) \quad B_1 = MB_2$$

$$(2viiiia) \quad \left[\frac{1}{2}MD^2 + \frac{1}{2} + D - c\right]\eta_1 + A_1 \cosh kD - B_1 \sinh kD - C_1 k D \cosh kD + D_1 k D \sinh kD = 0$$

$$(2ixia) \quad -\frac{M}{2k^2}\eta_1 + A_1 \cosh kD - B_1 \sinh kD - C_1 (\sinh kD + kD \cosh kD) + D_1 (\cosh kD + kD \sinh kD) = 0$$

$$(2xia) \quad -i\frac{M}{2k^2}c \cot \theta \eta_1 + A_1 \sinh kD - B_1 \cosh kD - C_1 k D \sinh kD + D_1 k D \cosh kD = 0.$$

This system of equations will have a non-trivial solution only if the determinant of its coefficients is equal to zero. The condition of vanishing determinant serves as the characteristic equation for  $c$ . By elimination of  $c$  between (2iii) and (2iv), it can be shown that the characteristic

equation is quadratic; for any specified  $k$ ,  $M$ ,  $D$ , and  $\theta$  there are exactly two roots (Loewenherz and Lawrence, 1988, in press). These two roots correspond to two different traveling wave modes, either of which may govern the stability of the flow.

The stability of the flow is determined by the imaginary parts of these roots, a positive imaginary part corresponding to an exponential growth  $\exp[k\text{Im}(c)t]$ . Neutral stability, characterized by the condition  $\text{Im}(c) = 0$ , describes a surface in the space of parameters  $k$ ,  $M$ , and  $D$  delimiting the regions of stability. Results indicate that the neutral stability locus is independent of  $\theta$ . Figure 2 shows the neutral stability curves obtained numerically after

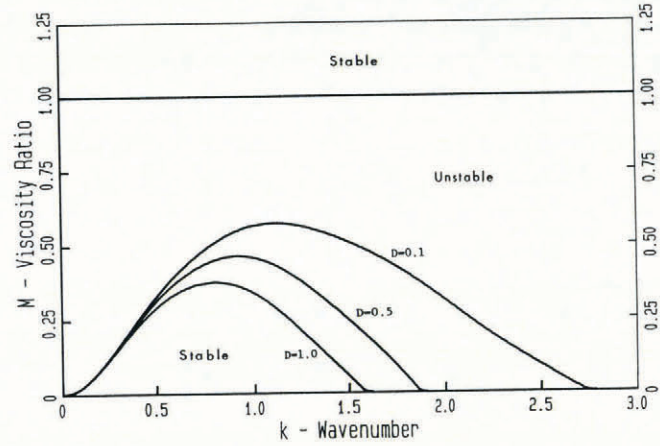


Fig. 2. Stability diagram for two-fluid layer model.

reduction to a  $5 \times 5$  system. Both of the axes  $k = 0$  and  $M = 0$  represent curves of neutral stability for all values of  $D$ , as does the line at  $M = 1$ . The remaining neutral curves indicated in Figure 2 divide regions of stability from those of instability in  $k - M$  space for the values of  $D$  specified. The results indicate that for  $M$  less than unity and all non-zero values of  $D$  instability is present in the long-wavelength limit. Additionally, for all values of the viscosity ratio  $M$  greater than unity (representing a fluid system in which the upper layer is less viscous than the lower layer), the configuration is linearly stable. Both of these results concur with those obtained previously by Kao (1968) using a long-wave approximation. However, it is also clear from the stability diagram, that instability is present at finite wave numbers for all values of  $D$  considered ( $D = 0.1-1.0$ ), and that, for viscosity ratios between about 0.5 and 1.0, the system is unstable at all finite wave numbers for that range of  $D$ . If ridge formation in rock glaciers is to be ascribed to these instabilities, it remains to ascertain how significant the instabilities are and at what wavelengths the fastest growing models will appear. In order to address this issue more fully, we must proceed to an examination of the growth rates associated with unstable waves.

An investigation of the  $D$ ,  $M$ ,  $k$ , and  $\theta$  parameter space indicates that, although the value of the wave number exhibiting the maximum growth rate shows little variation with respect to  $M$  and  $\theta$ , it does vary significantly with respect to  $D$ . These effects are partially demonstrated in Figure 3, which illustrates scaled growth rates as a function of the wave number for the specified values of  $D$  with  $M = 0.4$  and  $\theta = 0.2$ . (For a more detailed discussion of the parameter space, the reader is referred to the full set of results presented in Loewenherz and Lawrence (1988).) The imposed re-scaling is based on the total thickness of the rock glacier and the material velocity of the upper surface (which is approximately equal to the velocity of the unstable wave in the case of a thin layer), since these are readily observable quantities. As indicated in Figure 3, there are clearly two peaks in the growth rate as a function of  $k$  and this type of behaviour is apparent at all values of  $D$  and  $M$  considered. The peak associated with the faster growth rates is located in the region of greater wave numbers, and the wave number of the mode of faster growth is strongly dependent upon the thickness of the upper layer. As the thickness of the upper layer decreases,

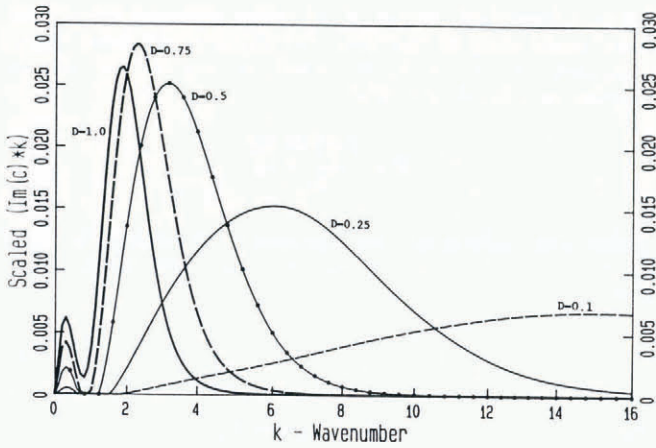


Fig. 3. Scaled growth rate as a function of  $k$  with  $M = 0.4$  and  $\theta = 0.2$ .

the value of the wave number exhibiting the maximum growth rate increases, scaling roughly with the inverse of  $D$ . Furthermore, the location of this major peak shows very little sensitivity to either  $\theta$  or  $M$ , although the magnitude of the growth rate does show substantial dependence on those parameters (Loewenherz and Lawrence, 1988, in press). We can, therefore, conclude that for the region of the parameter space of interest ( $M = 0.1-0.9$ ;  $D = 0.1-1.0$ ; and  $\theta = 0.1-1.5$ ), instability will be manifested in waves of wavelengths which are approximately three to four times the thickness of the upper layer. In the case of a rock glacier, this corresponds to wavelengths of 3–30 m or more, depending on one's estimate for the thickness of the upper layer of coarse material. This result generally agrees with reported rock-glacier ridge spacings (which are of the order of 2–50 m as mentioned above), suggesting that surficial ridge formation on rock glaciers may indeed be a product of viscosity stratification.

The actual growth rates associated with the flow instability, however, appear to be too slow for the formation of surficial ridges on rock glaciers independent of other mechanisms. Figure 4 illustrates the variation in the

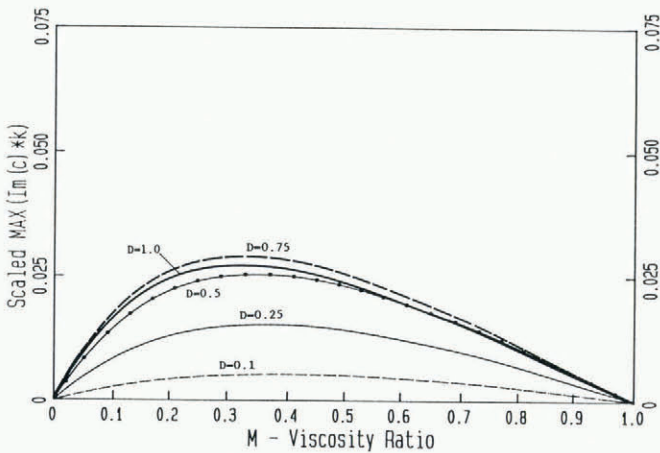


Fig. 4. Scaled maximum growth rate as a function of  $M$  with  $\theta = 0.2$  for values of  $D$  indicated.

maximum growth rate (determined by searching in  $k$ ) as a function of  $M$  for specified values of  $D$  with  $\theta = 0.2$  rad, and indicates that for all values of those parameters considered, the maximum growth rate occurs for a viscosity ratio of about 0.3. It should be noted that the scaled growth rates of these maximally unstable modes are small, i.e. never more than 0.03. Additionally, throughout the entire parameter space, growth rates are generally found to be of this order of magnitude. The value of 0.03 corresponds to a rate of growth of only 3% per unit of scaled time, which is the amount of time required for the rock glacier to creep down-slope through a distance equal

to its thickness. Therefore, the development of finite wave forms from an initially small disturbance would require a substantial amount of time, or alternatively, distance. More specifically, for a growth rate of 0.03, the rock glacier would have to flow a distance which is roughly equivalent to 30 times its thickness before the unstable wave forms would grow by even a factor of  $e$ . For a rock glacier exhibiting a thickness of 20–50 m, such a distance would be of the order of 500–2000 m, the latter of which exceeds the length of many rock glaciers.

It is possible that a decrease in the slope of the underlying incline could effectively amplify incipient instability, thereby producing waves of finite amplitude in the lee of the change in slope. This suggestion has been briefly considered by Loewenherz and Lawrence (1988), although a full analysis of the associated scattering problem has not been attempted. For the purposes of this discussion, however, the above results do allow us to conclude that a disturbance to the flow of a stratified system consisting of two fluid layers, in which the upper layer is more viscous than the lower layer, will be manifested in wave forms having wavelengths comparable to those observed on the surfaces of rock glaciers. The actual mechanisms associated with the amplification of a flow instability do, therefore, deserve further consideration.

### 3. THIN ELASTIC LAMINA MODEL

The mechanisms proposed in the literature for explaining the development of transverse ridges include the suggestion that the features develop in the presence of compression resulting from a decrease in the slope of the underlying incline (Wahrhaftig and Cox, 1959; Potter, 1972). This proposal, together with observations indicating stratification in the structure of a rock glacier, can be formulated in a precise model consisting of a thick viscous fluid substrate overlain by a thin elastic lamina. Since we characterize the upper layer as inextensible and retain the fluid flow model for describing the deformation of the entire configuration, a change in declivity necessarily produces differential movement within the system with a consequent development of compressive loads. Such compression, if of a sufficient magnitude, would be manifested as a buckling instability of the elastic lamina.

In order to develop the model, we will first consider the base flow of a single fluid layer in a semi-infinite domain,  $-L < x < \infty$ , which is supplied by a constant influx of material at  $x = -L$ . We will assume that a decrease in the slope of the incline occurs at  $x = 0$ , and that the regions away from  $x = 0$  are of constant slope. The behaviour of the system far from  $x = 0$  will be of particular interest, partly by virtue of its simplicity, but mostly inasmuch as it will provide the components for a global solution and will ultimately determine the manner in which compression develops in the surface lamina. After constructing a global base-flow solution, a stability analysis will be conducted by considering the stability of the global base flow in a region where the surficial compressive load and the slope of the underlying incline can be assumed to be approximately constant.

#### A. Global base flow

In the region of constant basal slope (either  $-L < x < 0$  or  $0 < x < \infty$ ), the governing equations are similar to those presented in the previous section. However, the upper layer of fluid must now be replaced with appropriate boundary conditions which represent the effects of the thin surface lamina and are applied at  $y = \xi$  (see Fig. 5). These new conditions require no slip at the upper surface due to the presence of the lamina and additionally specify the continuity of the traction on the lamina, i.e.

$$u = V \quad \text{at } y = \xi \quad (3.1)$$

and

$$n \cdot \sigma = \tau \quad \text{at } y = \xi \quad (3.2)$$

where  $V$  is the dimensionless material velocity of the lamina,  $\sigma$  is the stress tensor in the fluid and  $\tau$  is the

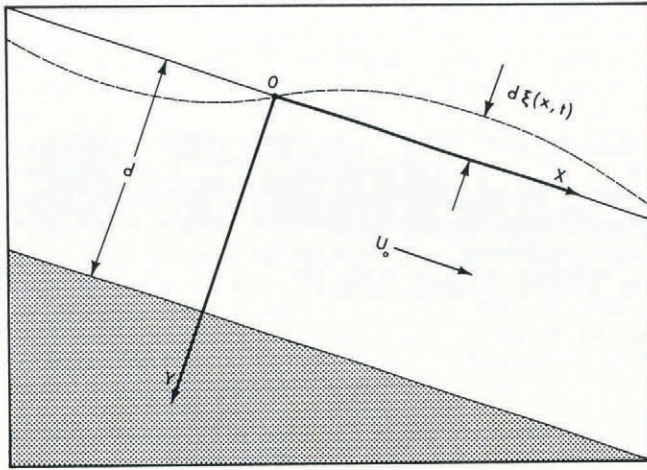


Fig. 5. Coordinate system for elastic lamina model.

dimensionless stress on the lamina. The kinematic interface continuity condition is retained in the form

$$\frac{DF}{Dt} = 0 \quad \text{at } y = \xi \tag{3.3}$$

as is the no-slip condition at the bottom, i.e.

$$u = v = 0 \quad \text{at } y = 1. \tag{3.4}$$

In the case of the base flow, we can assume that  $\xi = 0$ ,  $V = Ve_x$ , and  $\tau = e_x T_{,x}$  where  $T$  is the dimensionless tension per unit width of the lamina (scaled with  $\rho g d^2 \sin \theta$ ). The solution for the base flow can be readily obtained and is of the form

$$\begin{aligned} u &= \left[ V + \frac{1}{2}y \right] (1 - y) \\ v &= 0 \\ p &= \cot \theta y \\ T_{,x} &= V - \frac{1}{2} \end{aligned} \tag{3.5}$$

where  $u$  and  $v$  refer to the dimensionless velocity components and  $p$  represents the dimensionless pressure field. It should be recognized that had a lamina velocity of  $V = \frac{1}{2}$  been imposed, no tension or compression would develop. This case represents what might be thought of as the "natural" state of a fluid layer overlain by a thin elastic plate. We are, however, interested in the general case  $V \neq \frac{1}{2}$ , which corresponds to the differential movement of the layers.

We can construct a global solution by considering the case in which the underlying slope exhibits a decrease in declivity, and by assuming that there is no tension in the lamina at the up-stream point of origin of the flow and that at large distances down-stream, below the decrease in slope, the tension in the lamina is constant. These assumptions imply that the velocity of the lamina in the down-stream part of the flow must be consistent with the "natural" velocity of the down-stream flow field, so that the tension in the lamina is bounded in the far down-stream limit. It is expected that stress will be generated in the lamina as it passes through the region of variable slope. Using  $a$  and  $b$  to refer respectively to points far up-stream and down-stream from the region of variable slope, and invoking a constraint requiring a constant discharge through the system, an equation relating the up-stream and down-stream regions of the flow is obtained, i.e.

$$\frac{\hat{V} d_a}{2} + \frac{\rho g d_a^3 \sin \theta_a}{12\mu} = \frac{\hat{V} d_b}{2} + \frac{\rho g d_b^3 \sin \theta_b}{12\mu} \tag{3.6}$$

where dimensional forms of variables (denoted by  $\hat{\quad}$ ) are now being used to facilitate the physical argument being presented. As  $\hat{V}$  must be equal to the natural lamina velocity at point  $b$ , we have

$$\hat{V} = \frac{\rho g d_b^2 \sin \theta_b}{2\mu} \tag{3.7}$$

which when substituted into Equation (3.6) produces a cubic equation for the ratio of the up-stream and down-stream depths

$$\left[ \frac{d_a}{d_b} \right]^3 + \frac{\sin \theta_b}{\sin \theta_a} \left[ 3 \frac{d_a}{d_b} - 4 \right] = 0. \tag{3.8}$$

This equation has one real root given by

$$\frac{d_a}{d_b} = S^{1/3} \left[ \left[ (S + 4)^{1/2} + 2 \right]^{1/3} - \left[ (S + 4)^{1/2} - 2 \right]^{1/3} \right] \tag{3.9}$$

where  $S$  reflects the relative change in the angle of inclination

$$S = \frac{\sin \theta_b}{\sin \theta_a}. \tag{3.10}$$

As in Equation (2.1), the velocity scale  $U$  is proportional to the square of the depth and to the sine of the angle of bed inclination; therefore, the ratio of up-stream and down-stream velocity scales is given by

$$\frac{U_a}{U_b} = \left[ \frac{d_a}{d_b} \right]^2 \frac{1}{S}. \tag{3.11}$$

Furthermore, because the lamina is assumed inextensible, its material velocity must be identical in both the up-stream and down-stream regions of the flow field. Therefore, the dimensionless lamina velocities must be in a ratio inverse to that given in Equation (3.11). As the dimensionless lamina velocity is based on down-stream quantities, corresponding to the natural velocity there, the dimensionless velocity based on up-stream quantities is:

$$V_a = \left[ \frac{d_b}{d_a} \right]^2 \frac{S}{2}. \tag{3.12}$$

If  $S$  is close to unity,  $V_a$  is approximately

$$V_a = \frac{1}{2} + \frac{1}{3}(S - 1). \tag{3.13}$$

For a decrease in slope, i.e. when  $S < 1$ ,  $V_a$  will be less than  $\frac{1}{2}$ . Referring to Equation (3.5), it can therefore be concluded that in the region  $-L < x < 0$ , compression increases as one moves down-stream, and that compression develops to a maximum value of order  $\frac{1}{3}(1 - S)L$ , where  $L$  is the extent of the up-stream part of the rock glacier, scaled by the depth.

**B. Stability analysis**

Having presented a base-flow field which exhibits the development of compression, the issue arises as to whether that flow is stable against the buckling of its surface layer. A linear stability analysis of the base flow as described in Equation (3.5), with an assumed compressive load in the surface layer, is therefore indicated. As in section 2, the equation governing the stability of the perturbed flow field is

$$\nabla^4 \psi = 0 \tag{3.14}$$

where  $\psi$  is again the stream function for the perturbation to the base-velocity field. The conditions which are applied

to the perturbed flow field at the lower boundary are the kinematic no-slip conditions given by

$$(3i) \quad u = \psi_{,y} = 0 \quad \text{at } y = 1$$

$$(3ii) \quad v = -\psi_{,x} = 0 \quad \text{at } y = 1.$$

The kinematic interface continuity condition (3.1) when linearized to first order in  $\epsilon$  is

$$(3iii) \quad \left[ \frac{1}{2} - V \right] \xi + \psi_{,y} = 0 \quad \text{at } y = 0.$$

A normal stress condition can be derived from Equation (3.2) of the general form

$$n \cdot \sigma \cdot n = B_e \xi_{,xxxx} - (T \xi_{,x})_{,x} \quad (3.15)$$

where  $B_e$  is the dimensionless bending stiffness of the lamina (scaled with  $\rho g d^3 \sin \theta$ ). More specifically, upon evaluating the components of the stress tensor  $\sigma$ , this condition becomes

$$(3iv) \quad (T \xi_{,x})_{,x} - B_e \xi_{,xxxx} = \xi \cot \theta + p' + 2\psi_{,xy} + 2\xi_{,x} \left[ \frac{1}{2} - V \right] \quad \text{at } y = 0$$

when simplified to include only those terms which are linear in  $\epsilon$ . The kinematic condition (3.3) defining the surface displacement takes a form which is similar to that used in section 2, i.e.

$$(3v) \quad \xi_{,t} + V \xi_{,x} = -\psi_{,x} \quad \text{at } y = 0$$

In order to transform the equations using a Fourier integral, it must additionally be assumed that the unperturbed tension in the plate may be approximated by a constant. It is thus being posited that variations in the tension occur over a much larger length scale than that associated with the perturbed flow field. This assumption can be justified *a posteriori*. The transformed boundary conditions are

$$(3ia) \quad \phi' = 0 \quad \text{at } y = 1$$

$$(3iia) \quad \phi = 0 \quad \text{at } y = 1$$

$$(3iiia) \quad \frac{1}{2} - V \phi + \phi' = 0 \quad \text{at } y = 0$$

$$(3iva) \quad \left[ \cot \theta + 2ik \left[ \frac{1}{2} - V \right] + k^2 T + k^4 B_e \right] \frac{\phi}{c - V} = -3ik\phi' + \frac{i}{k} \phi'' \quad \text{at } y = 0$$

where the perturbed pressure has been eliminated from the equations by the use of a form of the governing equation similar to that given in Equation (2.18), and where the transformed displacement  $\eta(k)$  has been eliminated by considering the transform of condition (3v) above. A general solution to the governing Equation (3.14) is of the form

$$\phi = A \cosh ky + B \sinh ky + C k y \cosh ky + D k y \sinh ky \quad (3.16)$$

The dispersion relation associated with the perturbed field is then obtained by evaluating the determinant of the following system of linear equations:

$$\begin{aligned} & A \sinh k + B \cosh k + C(k \sinh k + \cosh k) + \\ & + D(k \cosh k + \sinh k) = 0 \\ & A \cosh k + B \sinh k + C k \cosh k + D k \sinh k = 0 \end{aligned} \quad (3.17)$$

$$A \left[ \frac{1}{2} - V \right] + Bk + Ck = 0$$

$$\frac{A}{c - V} \left[ \cot \theta + 2ik \left[ \frac{1}{2} - V \right] + k^2 T + k^4 B_e \right] + 2ik^2 B = 0.$$

The determinant of the above system will vanish if

$$c = V + \frac{(\frac{1}{2} - V)(2k \sinh^2 k) - iW(\sinh^2 k - k^2)}{2k^2(k + \sinh k \cosh k)} \quad (3.18)$$

where  $W$  has been defined as

$$W \equiv \cot \theta + k^2 T + k^4 B_e \quad (3.19)$$

As  $\sinh^2 k$  is always greater than or equal to  $k^2$  for all  $k$ , the system will be linearly stable if and only if  $W$  is greater than zero. Furthermore, since both  $\cot \theta$  and the bending stiffness  $B_e$  are positive, instability can occur only if  $T$  is negative, i.e. when the surface lamina is under compression.

The results indicate that, if the magnitude of the compression developed in the surface lamina exceeds a critical value, the upper surface of the fluid system should exhibit buckling. This critical tension can be obtained by minimizing  $W$  with respect to  $k^2$ ,

$$\frac{\partial W}{\partial k^2} = 0 \quad (3.20)$$

which allows the identification of the wave number,  $k_{\min}$ , associated with the least stable (or most unstable) mode, i.e.

$$k_{\min} = \left[ -\frac{T}{2B_e} \right]^{\frac{1}{2}} \quad (3.21)$$

$W$  is negative at that point if

$$T \leq T_c = -(4B_e \cot \theta)^{\frac{1}{2}} \quad (3.22)$$

where  $T_c$  is the critical tension associated with the onset of instability. The critical wavelength,  $\lambda_c$ , of this instability is then given by Equation (3.21) evaluated at the critical tension,

$$\lambda_c = \frac{2\pi}{k_{\min}} = 2\pi \left[ -\frac{2B_e}{T_c} \right]^{\frac{1}{2}} = 2\pi \left[ \frac{B_e}{\cot \theta} \right]^{\frac{1}{4}} \quad (3.23)$$

This represents the wavelength which will be observed in the surface buckling. The distance,  $x_c$ , necessary to develop the critical compressive load from an initial load of zero in the base flow can be estimated as

$$x_c = \frac{T_c}{T_{,x}} = \frac{(4B_e \cot \theta)^{\frac{1}{2}}}{\frac{1}{2} - V} \quad (3.24)$$

where the base-flow solution for the tension given by Equation (3.5) has been used. In dimensional form the three critical quantities are given by

$$\hat{T}_c = -2(\hat{B}_e \rho g \cos \theta)^{\frac{1}{2}} \quad (3.25)$$

$$\hat{\lambda}_c = 2\pi \left[ \frac{\hat{B}_e}{\rho g \cos \theta} \right]^{\frac{1}{4}} \quad (3.26)$$

$$\hat{x}_c = \frac{2}{d \left[ \frac{1}{2} - V \right] \sin \theta} \left[ \frac{\hat{B}_e \cos \theta}{\rho g} \right]^{\frac{1}{2}} \quad (3.27)$$

For a thin plate, the bending stiffness,  $\hat{B}_e$ , is evaluated using the plane-strain formula, which for the purposes of this analysis can be approximated by

$$\hat{B}_e = \frac{Et_h^3}{12} \tag{3.28}$$

where  $E$  is the Young's modulus of the elastic lamina and  $t_h$  is its thickness. We introduce units which are chosen so that the rock-glacier parameters have numerical values of order unity, i.e. the Young's modulus is scaled in units of  $10^8$  Pa

$$E = E_8 \times 10^8 \text{ Pa,}$$

the flow depth in units of 20 m

$$d = d_{20} \times 20 \text{ m,}$$

the lamina thickness in units of 1 m

$$t_h = t_1 \text{ m,}$$

and the density in units of 2500 kg/m<sup>3</sup>

$$\rho = \rho_{2.5} \times 2500 \text{ kg/m}^3.$$

The expressions for the critical tension, wavelength, and distance become

$$\hat{T}_c = -10^6 (\cos \theta)^{1/2} E_8^{1/2} \rho_{2.5}^{1/2} \text{ N/m}$$

$$\hat{\lambda}_c = 30 (\cos \theta)^{-1/4} E_8^{3/4} \rho_{2.5}^{-1/4} \text{ m}$$

$$\hat{x}_c = \frac{2(\cos \theta)^{1/2}}{\sin \theta \left[ \frac{1}{2} - V \right]} E_8^{1/2} \rho_{2.5}^{-1/2} d_{20}^{-1} \text{ m.}$$

The selection of a value for Young's modulus is speculative and represents the most uncertain parameter specified. Due to the paucity of adequate data regarding the material properties of a rock/ice composite, it is difficult to make a reliable estimate.  $10^8$  Pa is much less than that commonly associated with pure rock and reflects the relatively loose packing of the upper layer. Based on the above estimates for rock-glacier parameters, one can conclude that, for a change in slope of about 20% on a plane inclined at 0.2 rad, the critical distance for developing a compressive load sufficient to cause buckling is on the order of 100 m from the origin of the rock glacier to its decrease in slope, which is well within the range of observed rock-glacier extents. The wavelength associated with that buckling would be, for lamina thicknesses of 1–3 m, on the order of 30–70 m, which is roughly within the range of observed ridge spacings. For a Young's modulus of  $10^7$  Pa, these estimates would be reduced by a factor of two. These values are based on rather crude estimates, but nonetheless indicate that it is possible to develop compressive loads within rock glaciers which are capable of generating surface instabilities, and that the finite wave forms arising from that instability will have wavelengths which are similar to those observed in the field. A full analysis of rock-glacier development based on this model would require more complete information regarding the material properties of a rock/ice composite medium than is presently available.

#### 4. CONCLUSIONS

In a single-layer, free surface flow at low Reynolds numbers is known to be stable to small perturbations (Yih, 1963; Thompson, 1979), so that neither of the instabilities discussed herein could be present in the rock-glacier flow models suggested by Wahrhaftig and Cox (1959) or more recently by Olyphant (1983). Based on those models, one might negatively conclude that transverse surficial ridges can only be derived from periodic variations in debris supply or other external forcing to the system. The two models

proposed in this paper, though, provide more realistic representations of rock-glacier structure than do the single-layer models in that they characterize the stratified nature of rock-glacier forms. Furthermore, the results of our linear-stability analyses clearly imply that this stratification can generate instabilities which would be manifested in surficial wave forms. Both of the instabilities identified (i.e. the flow instabilities associated with the two-fluid layer model and the buckling instability in the elastic lamina case) will occur in the absence of climatically driven variations in source material. Thus, the results provide strong support for the suggestion made by Ives (1940) that transverse surficial ridges are the product of the differential movement of discrete layers of debris. Additionally, in the case of the elastic lamina model, our analysis indicates that a decrease in the slope of the underlying incline contributes to the development of a compressive load in the upper surface, which is necessary for surface buckling. This latter result tentatively verifies assessments by Wahrhaftig and Cox (1959) and more recently by Potter (1972) that surface ridges are generated as a product of "compression" induced in the flow field via a change in the slope of the underlying surface. However, further constitutive modelling which is based on field data and laboratory experimentation and is designed to characterize the viscosity of rock-glacier material as a function of particle size and temperature is necessary in order to assess completely the factors determining rock-glacier rheology.

With respect to the long-term development of rock-glacier forms, the two models illustrate that transverse ridges can develop under conditions of constant debris influx. This has significant implications concerning the feasibility of employing rock-glacier forms in the reconstruction of paleoclimatic conditions. It has been proposed that active rock glaciers could provide information regarding variations in climatic conditions throughout the Holocene (Hassing and Mayewski, 1983; Olyphant, 1987; Thorn and Loewenherz, 1987). In principle, this seems quite likely as many of the large, active rock glaciers are at least 3500 and may be up to 10 000 years old (Haeblerli and others, 1979; Evin and Assier, 1982). However, from our analyses, it is clear that visible perturbations on the surface of a rock glacier are not necessarily solely a product of fluctuations in debris supply. In fact, it is quite likely that spatially periodic transverse ridges develop as a result of either or both of the internal mechanisms considered herein, and that variations in external forcing arising from climatically driven rates of debris production would be manifested on a larger scale and thus are superimposed on the instability of the flow configuration. If this is the case, then the use of rock-glacier forms in a detailed reconstruction of Holocene climatic conditions may be much more difficult than has been anticipated. A thorough identification of the relative roles of climatic forcing versus rheologically derived instability and the response time of the rock-glacier form to either of these mechanisms would be necessary before such a task could be seriously considered.

#### REFERENCES

- Barsch, D. 1977. Nature and importance of mass-wasting by rock glaciers in Alpine permafrost environments. *Earth Surface Processes*, 2(2–3), 231–245.
- Barsch, D. 1987. The problem of the ice-cored rock glacier. In Giardino, J., J. Schroder, jr, and J. Vitek, eds. *Rock glaciers*. Boston, etc., Allen and Unwin, 45–53.
- Barsch, D. 1988. Rockglaciers. In Clark, M.J., ed. *Advances in periglacial geomorphology*. Chichester, NY, John Wiley and Sons, 69–90.
- Barsch, D., H. Fierz, and W. Haeblerli. 1979. Shallow core drilling and bore-hole measurements in the permafrost of an active rock glacier near the Grubengletscher, Wallis, Swiss Alps. *Arct. Alp. Res.*, 11(2), 215–228.
- Benedict, J.B. 1973. Correspondence. Origin of rock glaciers. *J. Glaciol.*, 12(66), 520–522.
- Benedict, J.B., R.J. Benedict, and D. Sanville. 1986. Arapaho rock glacier, Front Range, Colorado, U.S.A.: a 25-year resurvey. *Arct. Alp. Res.*, 18(3), 349–352.

- Benjamin, T.B. 1957. Wave formation in laminar flow down an inclined plane. *J. Fluid Mech.*, 2, 554-574.
- Birkeland, P.W. 1973. Use of relative age-dating methods in a stratigraphy study of rock glacier deposits, Mt. Sopris, Colorado. *Arct. Alp. Res.*, 5(4), 401-416.
- Blagbrough, J.H. and S.E. Farkas. 1968. Rock glaciers in the San Mateo Mountains, south-central New Mexico. *Am. J. Sci.*, 266, 812-823.
- Brown, W.H. 1925. A probable fossil glacier. *J. Geol.*, 33, 464-466.
- Calkin, P.E., L.A. Haworth, and J.M. Ellis. 1987. Rock glaciers of central Brooks Range, Alaska, U.S.A. In Giardino, R.J., J.F. Schroder, jr, and J.D. Vitek, eds. *Rock glaciers*. Boston, etc., Allen and Unwin, 65-82.
- Chaix, A. 1923. Les coulées de blocs du Parc National Suisse d'Engadine. *Globe (Organe de la Société de Géographie de Genève)*, 62, 1-38.
- Corte, A.E. 1976. Rock glaciers. *Biul. Periglac.*, 26, 175-197.
- Evin, M. and A. Assier. 1982. Mise en évidence du mouvement sur le glacier rocheux du Pic d'Asti (Queyras, Alpes du Sud, France). *Rev. Géomorphol. Dyn.*, 31, 127-136.
- Fisch, W., sr, W. Fisch, jr, and W. Haerberli. 1978. Electrical D.C. resistivity soundings with long profiles on rock glaciers and moraines in the Alps of Switzerland. *Z. Gletscherkd. Glazialgeol.*, 13(1-2), 1977, 239-260.
- Haerberli, W., L. King, and A. Flotron. 1979. Surface movement and lichen-cover studies at the active rock glacier near the Grubengletscher, Wallis, Swiss Alps. *Arct. Alp. Res.*, 11(4), 421-441.
- Harris, S.A. 1981. Distribution of active glaciers and rock glaciers compared to the distribution of permafrost landforms, based on freezing and thawing indices. *Can. J. Earth Sci.*, 18(2), 376-381.
- Hassinger, J.M. and P.A. Mayewski. 1983. Morphology and dynamics of the rock glaciers in southern Victoria Land, Antarctica. *Arct. Alp. Res.*, 15(3), 351-368.
- Ives, R.L. 1940. Rock glaciers in the Colorado Front Range. *Geol. Soc. Am. Bull.*, 51, 1271-1294.
- Johnson, P.G. 1981. The structure of a talus-derived rock glacier deduced from its hydrology. *Can. J. Earth Sci.*, 18(9), 1422-1430.
- Kao, T.W. 1968. Role of viscosity stratification in the stability of two-layer flow down an incline. *J. Fluid Mech.*, 33, 561-572.
- Kesseli, J.E. 1941. Rock streams in the Sierra Nevada, California. *Geogr. Rev.*, 31(2), 203-227.
- King, L., W. Fisch, W. Haerberli, and H.P. Waechter. 1987. Comparison of resistivity and radio-echo soundings on rock glacier permafrost. *Z. Gletscherkd. Glazialgeol.*, 23(1), 77-97.
- Lliboutry, L. 1953. Correspondence. Internal moraines and rock glaciers. *J. Glaciol.*, 2(14), 296.
- Loewenherz, D.S. and C.J. Lawrence. 1988. *Stability of viscous stratified free surface flows at low Reynolds number with reference to the modelling of rock glaciers*. Urbana, IL, University of Illinois. (T. & A.M. Report 488.)
- Loewenherz, D.S. and C.J. Lawrence. In press. The effect of viscosity stratification on the stability of a free surface flow at low Reynolds number. *Phys. Fluids*.
- Luckman, B.H. and K.J. Crockett. 1978. Distribution and characteristics of rock glaciers in the southern part of Jasper National Park, Alberta. *Can. J. Earth Sci.*, 15(4), 540-550.
- Madole, R. 1972. Neoglacial facies in the Colorado Front Range. *Arct. Alp. Res.*, 4(2), 119-130.
- Mahaney, W.G. 1980. Late Quaternary rock glaciers, Mount Kenya, Kenya. *J. Glaciol.*, 25(93), 492-497.
- Mayewski, P.A. and J. Hassinger. 1981. Characteristics and significance of rock glaciers in southern Victoria Land, Antarctica. *Antarct. J. U.S.*, 15(5), 1980, 68-69.
- Mayewski, P.A., P.A. Jeschke, and N. Ahmad. 1981. An active rock glacier, Wavbal Pass, Jammu and Kashmir Himalaya, India. *J. Glaciol.*, 27(95), 201-202.
- Morris, S.E. 1981. Topoclimatic factors in the development of rock glacier facies, Sangre de Cristo Mountain, southern Colorado. *Arct. Alp. Res.*, 13(4), 329-338.
- Olyphant, G.A. 1983. Computer simulation of rock-glacier development under viscous and pseudoplastic flow. *Geol. Soc. Am. Bull.*, 94(4), 499-505.
- Olyphant, G.A. 1985. Topoclimate and the distribution of neoglacial facies in the Indian Peaks section of the Front Range, Colorado, U.S.A. *Arct. Alp. Res.*, 17(1), 69-78.
- Olyphant, G.A. 1987. Rock glacier response to abrupt changes in talus production. In Giardino, J., J. Schroder, jr, and J. Vitek, eds. *Rock glaciers*. Boston, etc., Allen and Unwin, 55-64.
- Outcalt, S.I. and J.B. Benedict. 1965. Photo-interpretation of two types of rock glacier in the Colorado Front Range, U.S.A. *J. Glaciol.*, 5(42), 849-856.
- Potter, N., jr. 1972. Ice-cored rock glacier, Galena Creek, northern Absaroka Mountains, Wyoming. *Geol. Soc. Am. Bull.*, 83(10), 3025-3057.
- Richmond, G.M. 1952. Comparison of rock glaciers and block streams in the La Sal Mountains, Utah. *Geol. Soc. Am. Bull.*, 63, 1292-1293.
- Thompson, D.E. 1979. Stability of glaciers and ice sheets against flow perturbations. *J. Glaciol.*, 24(90), 427-441.
- Thorn, C.E. and D.S. Loewenherz. 1987. Spatial and temporal trends in alpine periglacial studies: implications for paleo reconstruction. In Boardman, J., ed. *Periglacial processes and landforms in Britain and Ireland*. Cambridge, etc., Cambridge University Press, 57-65.
- Wahrhaftig, C. and A. Cox. 1959. Rock glaciers in the Alaska Range. *Geol. Soc. Am. Bull.*, 70(4), 383-436.
- Whalley, W.B. 1974. *Rock glaciers and their formation as part of a glacier debris-transport system*. Reading, University of Reading. (Reading Geographical Papers 24.)
- White, S.E. 1971. Rock glacier studies in the Colorado Front Range, 1961 to 1968. *Arct. Alp. Res.*, 3(1), 43-64.
- White, S.E. 1975. Additional data on Arapaho rock glacier in the Colorado Front Range, U.S.A. *J. Glaciol.*, 14(72), 529-530.
- White, S.E. 1976. Rock glaciers and block fields, review and new data. *Quat. Res.*, 6(1), 77-97.
- White, S.E. 1981. Alpine mass movement forms (non-catastrophic): classification, description, and significance. *Arct. Alp. Res.*, 13(2), 127-137.
- Yih, C.-S. 1963. Stability of liquid flow down an inclined plane. *Phys. Fluids*, 6, 321-334.

MS. received 3 December 1988 and in revised form 12 April 1989